International Journal of Emerging Science and Engineering (IJESE)
ISSN: 2319–6378, Volume-1, Issue-12, October 2013

Noise Reduction in Hyperspectral Images Through Spectral Unmixing

Milad Razmi, Ali Rafiee, Zoheir Kordrostami

Abstract*— Spectral unmixing and denoising of hyperspectral images have always been regarded as separate problems. By considering the physical properties of a mixed spectrum, this letter introduces unmixing-based denoising, a supervised methodology representing any pixel as a linear combination of reference spectra in a hyperspectral scene. Such spectra are related to some classes of interest, and exhibit negligible noise influences, as hey are averaged over areas for which ground truth is available. After the unmixing process, the residual vector is mostly composed by the contributions of uninteresting materials, unwanted atmospheric influences and sensor-induced noise, and is thus ignored in the reconstruction of each spectrum. The proposed method, in spite of its simplicity, is able to remove noise effectively for spectral bands with both low and high signal-to-noise ratio. Experiments show that this method could be used to retrieve spectral information from corrupted bands, such as the ones placed at the edge between ultraviolet and visible light frequencies, which are usually discarded in practical applications. The proposed method achieves better results in terms of visual quality in comparison to competitors, if the mean squared error is kept constant. This leads to questioning the validity of mean squared error as a predictor for image quality in remote sensing applications.

Index Terms*— Denoising, hyperspectral images, image restoration, mean squared error, spectral unmixing.

I. INTRODUCTION

The SPECTRAL range characterizing data acquired by state-of-the-art hyperspectral sensors mostly spans the frequencies between 400 and 2500 nm. Some sensors, such as the Airborne Visible/InfraRed Imaging Spectrometer (AVIRIS) and the future HySpiri mission, also acquire data in the portion of the spectrum that is placed at the edge between near ultraviolet (NUV) frequencies and visible light (380–400 nm) [1]. The spectral bands in this range are affected by noise coming from several sources, and therefore difficult to model [2]. Such bands are typically characterized by a low signal-tonoise ratio (SNR), and as a consequence are usually discarded in a preprocessing step common to most practical applications. For some specific tasks, it would be desirable to keep such spectral information; a typical example is the study of colored dissolved organic matter (CDOM) in natural waters CDOM inhibits phytoplankton productivity by absorbing UV and NUV radiation, affecting in turn remote estimates of clorophyll concentration [3]. As the bands in the NUV-blue portion of the spectrum are usually noisy and therefore difficult to interpret, bands at longer wavelengths characterized by a better SNR are usually preferred to derive empirical indices for its estimation. As an example, Johannessen *et al.* [4]simulated the reflectance at 380 nm using the bands in the 400–500 nm portion of the spectrum. Therefore, a specific denoising methodology enabling a direct use of the information in the mentioned spectral range would represent a great aid for such applications.

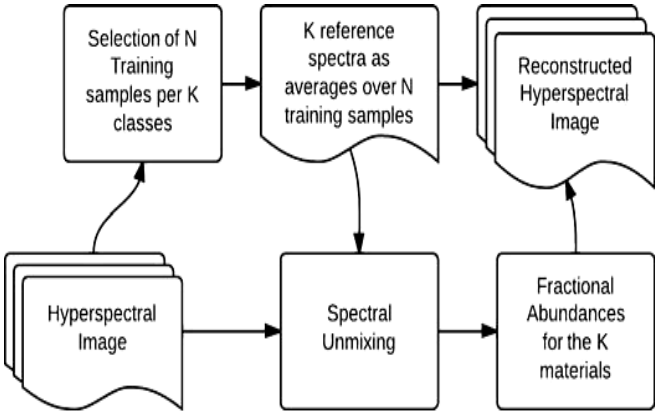

Fig. 1. Workflow for unmixing-based denoising.

The selected reference spectra are averaged over a given area of interest, which is homogeneous to some degree, and the image is reconstructed as a linear combination of the reference spectra. The residual of the unmixing process is discarded along with most of the noise in the data.

Denoising is often carried out in image processing through filtering, usually based on convolutions with sliding windows in the image domain, on operations in the frequency domain, or on estimated noise statistics or degradation functions, if these are known for the image acquisition process [5]. In the case of hyperspectral images, the high dimensionality of the data and the correlation between adjacent bands can be exploited to carry out effective denoising procedures based on dimensionality reduction (DR) algorithms, which project the data onto a subspace where meaningful information is preserved, while noise and some high frequencies are discarded [6], [7]. The often preferred DR technique is the Minimum Noise Fraction (MNF) [8], and the problems arising from the use of this method have been seldom addressed. First, MNF needs the number of noisy components to be estimated, which is not a trivial problem [9]. In addition, this estimation is different for bands with different SNR, as it is not possible to achieve an optimal denoising for all the bands at the same time. Finally, the usual way of validating the quality of the denoised images

Manuscript Received on October 2013.

Milad Razmi, Department of Electrical Engineering, Branch Bushehr slamic Azad University, Bushehr, Iran.

Ali Rafiee, Electrical Engineering Department Kazeroun Branch Islamic Azad University, Kazeroun, Iran.

Zoheir Kordrostami, Department of Electrical Engineering, Shiraz University of Technology, Shiraz, Iran

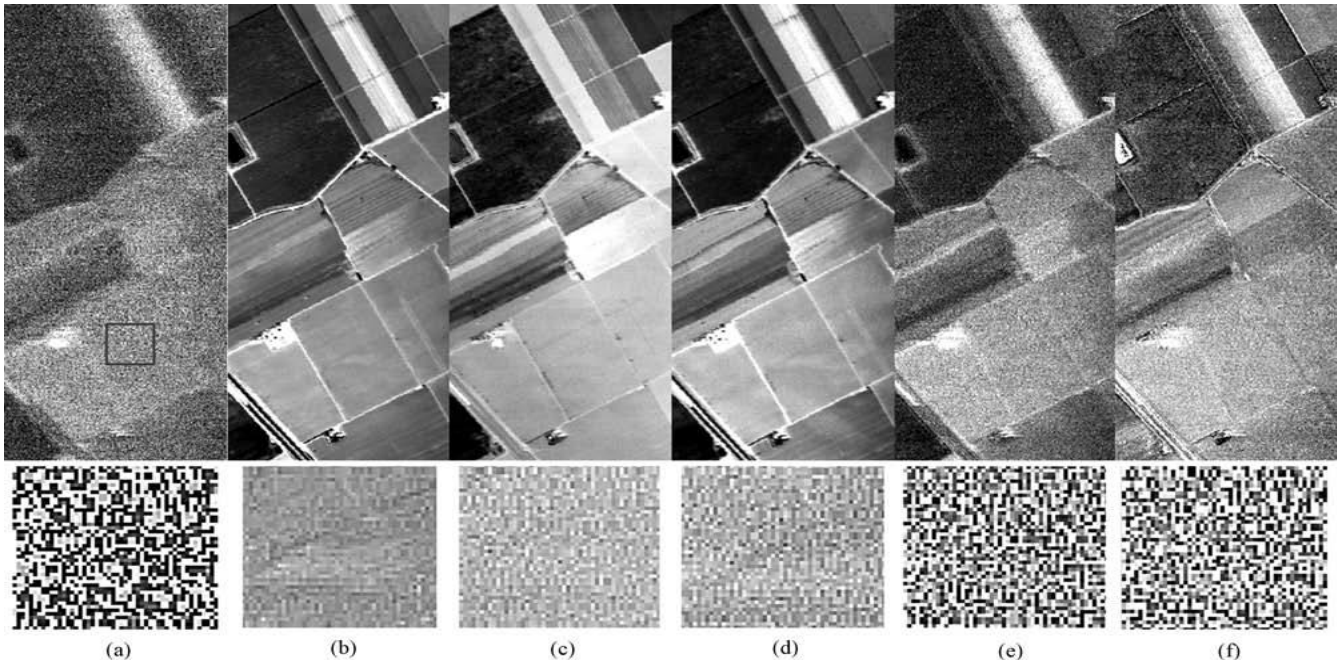

Fig. 2. Band at 380 nm. (a) Original image. (b) Reconstruction obtained with UBD using NNLS unmixing. (c)–(e) Reconstructed images using 4, 7, and 30 MNF components, respectively. (f) Reconstruction obtained with UBD using NCLS unmixing. Below: magnified areas represented by the square in (a), after a high-pass filtering of the image to make the noise more evident.

in the literature is by computing the mean squared error (MSE) between original and reconstructed image, with MNF being optimal in a MSE sense, as it represents each band as a linear combination of other bands minimizing the MSE. This is also the case for other hyperspectral denoising algorithms driven by MSE minimization [10]. Nevertheless, in recent years, studies in image processing have shown that degraded images with constant MSE may exhibit very different visual image quality, and indices that capture statistical image properties related to human perception are becoming widely accepted in the image processing community to estimate distortions [11]. Therefore, validation techniques using MSE as a quality predictor may be biased. Nascimento and Bioucas Dias [12] explored the correspondences between another DR technique, the independent components analysis, and spectral unmixing [13], which aims at quantitatively decomposing each pixel in signals related to macroscopically pure materials, or endmembers. While the experiments in the aforementioned work are derived from a statistical analysis of the data, this letter introduces a supervised denoising algorithm based on spectral unmixing that results from considerations on the physical properties of a mixed pixel, which can be described as follows. In a first step, a set of reference spectra is derived by spatial averaging of neighboring pixels in each class of interest. Subsequently, each image element, considered as a mixed spectrum, is expressed as a linear combination of the reference spectra and a residual vector, which quantifies the unmixing error. If the considered reference spectra are noise-free and comprise all the relevant classes in the image, such a vector will mostly be composed by noise and components of less interest. Therefore, each full spectrum can be reconstructed ignoring the residual vector. Results obtained through the described unmixing-based denoising (UBD) algorithm show a superior visual image quality with respect to the reconstruction using MNF features, if the MSE is kept constant. The method works equally well for bands with high SNR, while a different number of components has to be kept in the inverse MNF rotation according to the band SNR. The reported experiments lead to questioning the validity of MSE as a quality predictor in applications to hyperspectral and, in general, remotely sensed data.

This letter is structured as follows. Section II introduces the proposed denoising methodology based on spectral unmixing. We report experimental results and comparison with MNF based denoising in Section III, and conclude in Section IV.

II. Unmixing-Based Denoising

A recently described classification methodology for hyperspectral data based on synergetics theory [14] projects any image element onto a semantic subspace, in which every dimension represents the similarity to a given class of interest. This procedure inspires a supervised methodology based on spectral unmixing. Given a hyperspectral image element m with p bands, and a training dataset containing n samples from each of k classes, with $k < p$, UBD is a simple procedure that can be described as follows. First, a set of reference spectra is defined as $A = \{x1, \ldots, xi, \ldots, xk\}$, where xi is the average of the n spectra belonging to class i. Considering the mean value for a given reference spectrum ensures that, if each class is spectrally homogeneous, the presence of noise in it is reduced to a minimum. Such assumptions are also made in [15], in which spectra averaged within some classes of interest are employed to perform a supervised spectral unmixing prior to classification. Even though no assumption on the purity of the reference spectra is made, the image elements belonging to a homogeneous area have a higher prior probability of being related to some pure material [16]. Afterward, any unmixing procedure can be employed to decompose the signal in a combination of the reference spectra. If we assume this to be

linear, we have

$$m = \sum_{i=1}^{k} x_i s_i + r \qquad (1)$$

where s_i is the fraction or abundance of the reference spectrum i in m, and r is residual vector. The latter can be expressed as

$$r = r_1 + r_2 + r_n \qquad (2)$$

where $r1$ is given to components related to materials not present in A, $r2$ is an error given by subtle variations of one or more materials in A, and rn is caused by atmospheric influence and instrument-induced noise. The noise here is regarded a additive, as a study in [2] concludes that signal-dependant noise in typical hyperspectral sensors can be neglected. If our classes of interest are well captured in A, we are not interested in other materials, and therefore, we can ignore $r1$, and if they are homogeneous we expect rn to be predominant over $r2$ for bands with low SNR. Therefore, we can derive a reconstruction $\hat{m}$ for a spectrum m as

$$\hat{m} = \sum_{i=1}^{k} x_i s_i \qquad (3)$$

ignoring r, and along with it most of the noise affecting m. The workflow is reported in Fig. 1. The described procedure is based on the assumption that if the contributions to the radiation reflected from a resolution cell are known, the value of noisy bands in that area can be derived by a combination of the average values characterizing each component in that spectral range. The proposed method is supervised and is carried out independently for each pixel. In addition, it assumes that the selected spectra in the scene are known or can reliably be estimated, and a certain homogeneity of the classes of interest, which is to be expected in a natural scene rather than in a scene where man-made objects are prevalent.

III. RESULTS

A. Salinas Dataset

We analyze an AVIRIS hyperspectral scene containing agricultural fields acquired over the Salinas Valley, USA, of size 512 × 217 pixels with 192 spectral bands from 0.38 to 2.5μm (water absorption bands removed as in [17]), and with a spatial resolution of 3.7 m. As expected, the band centered at 380 nm is severely affected by noise [Fig. 2(a)]. Ground truth is available for 15 classes in the area reported in Fig. 3(f), and we select the average spectrum over a 6 × 6 pixels area for each class (the size of the averaging window has been set empirically), resulting in 16 reference spectra (the class corn has been divided in two classes as in [14]).

As unmixing algorithm for (1) we adopt nonnegative least squares (NNLS), which has the advantage of being physically meaningful, as in its solution all abundances are positive [13]. In recent years, the fully constrained least-squares (FCLS) method, which enforces not only nonnegativity but also the sum-to-one constraint on the estimated abundances, has been debated by the community and is therefore not considered in these experiments [13]. The results for UBD using NNLS are reported in Figs. 2(b) and 3(b) for the bands at 380 and 750 nm, respectively. Both bands, characterized by a different SNR, exhibit high visual quality, while spectral distortions appear negligible. The normalized RMSE (NRMSE), expressed in percentage, is around 15% and 1.7% for these two bands, and in the second case, it drops down to 0.9% in the area for which ground truth was available, and from which the reference spectra were selected (Table I). A magnification of a high-pass filtered version of the images shows clean and smooth areas, suggesting that such distortions are mostly related to the noise that has been removed. If nonconstrained least squares (NCLS) unmixing is used instead of NNLS results are much degraded, as the physical assumptions made are no longer valid: Fig. 2(f) is still severely affected by noise and presents some very distorted areas. As an example, no reference spectrum has been selected for the small pond of water on the upperleft side of the image, which exhibits abnormally high values. It is of interest to make some comparison to the same image reconstructed using a subset of k MNF features. The problem of selecting the optimal number k affects most algorithms, as generally the representation of noise and relevant information in the MNF components presents a certain overlap, and the boundary between these is difficult to locate automatically [9]. In the literature, this is usually set with an empirical threshold based on the eigenvalues related to the features, on a visual inspection, or on quality indicators for analysis carried out in the MNF parameter space, such as classification accuracy. A procedure is proposed in [9] to estimate the optimal value for k by taking into account the dark current measured by the images acquired by a hyperspectral sensor with a closed shutter, and to validate the results by comparing the reconstructed images to some ideally noise-free images. These present some similarity with UBD, as they are achieved by applying NCLS unmixing using as input a spectral library and an unsupervised classification of an input reflectance image. Nevertheless, as this method uses external libraries containing spectra acquired in diverse conditions, it cannot be applied to reliably remove noise from a real image; in addition, the advantages of using NNLS over NCLS have just been discussed.

In these experiments, we choose to select the number of MNF feature k empirically to match the RMSE obtained with UBD, keeping in mind that RMSE is expected to decay as k grows. As no value of k yields a minimization both of the noise and of the spectral distortion across all the bands with varying SNR, we reconstruct the image with a varying number of MNF features.We match RMSE for the bands at 380 and 750 nm, for the whole band and in the area where ground truth is available [applying the mask in Fig. 3(f)]. The resulting values for k are 4, 7, and 30, respectively. All results are reported in Figs. 2 and 3 and in Table I. It is clear that the noise in the band at 380 nm increases with the number of MNF features used in the back rotation. On the other hand, the noise in the band a 750 nm decreases, but no reconstruction can provide an image as clean as the result of UBD, as noise starts already to affect the image with a reconstruction using few MNF components

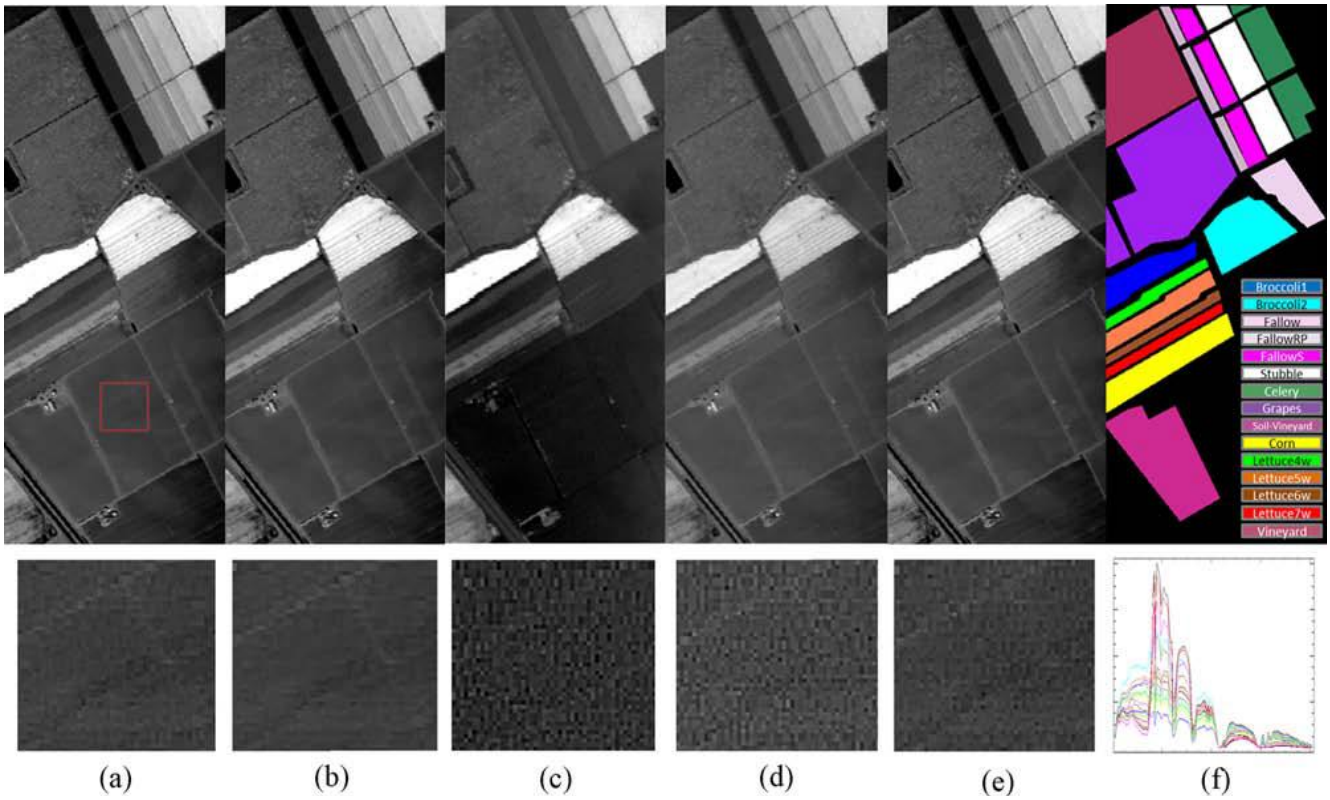

Fig. 3. Band at 750 nm. (a) Original image. (b) Reconstruction obtained with UBD using NNLS unmixing. (c)–(e) Reconstructed images using 4, 7, and 30 MNF components, respectively. (f) Areas in the image where ground truth is available. Bottom: (a)–(e) Magnified areas represented by the square in (a), after a high-pass filtering of the image to make the noise more evident. (f) Reference spectra collected from the ground truth.

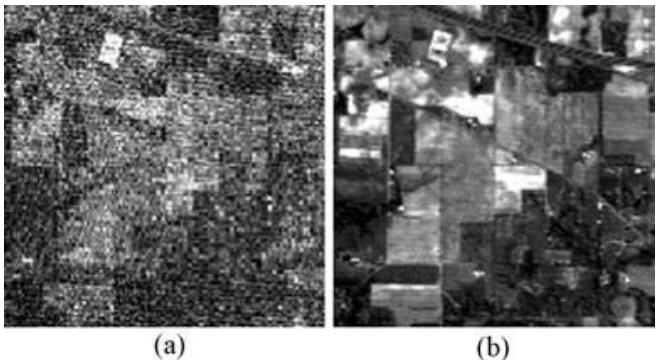

Fig. 4. (a) Single band centered at 370 nm from the Indian Pines dataset. (b) UBD results.

(namely 4). It may be argued that keeping more MNF features would reduce distortions, but it can be seen that increasing k in the back rotation severely affects the denoising of bands with low SNR [see Fig. 2(e)].

An interesting consideration to be done on this comparison is that the visual image quality is higher for UBD, for comparable values of RMSE. Fig. 2(c) present severe spectral distortions in comparison to UBD, while images in Fig. 3(d) and (e) are more noisy. In addition, some spectral information in Fig. 3(d) is visibly corrupted; for example, the bright fields in the center of the scene appear darker than in the original image in Fig. 3(a) (the histogram stretch is the same in all the images). Please note that RMSE is used in these experiments only as an empirical indicator to select a meaningful value for k, not as an evaluation metric. Indeed, our results suggest that RMSE could be a poor objective criterion to assess the image quality of remotely sensed data, as it has already been found to be for monochromatic and color pictures [11].

B. Indian Pines Dataset

A second experiment is carried out on the popular AVIRIS Indian Pines dataset, of size 145 × 145 and containing 224 bands. One reference spectrum has been collected from an averaged area of 5 × 5 pixels for each of the available 15 classes in the groundtruth image. We applied UBD to the full dataset and report in Fig. 4 the results for the first band of the dataset. The denoised image has a NRMSE of 3.6%, with a mean NRMSE value across all bands of 1.6%.

IV. CONCLUSION

Spectral unmixing and denoising algorithms for hyperspectral remote sensing were always considered independently. In this paper, we propose Unmixing-based Denoising (UBD), a methodology based on the physical rather than statistical properties of the components of a given spectrum: while traditional algorithms are based on second-order statistics, UBD reconstructs a single spectrum as a linear combination of noise-free reference spectra. This allows reconstructing bands with low SNR with a certain degree of reliability and represents a viable solution for the recovery of junk bands, which are usually discarded in practical applications. A drawback of the method is that it requires either prior knowledge of the scene, or a reliable identification of the classes of interest in the image. Furthermore, it needs a reasonably large number of pixels for each reference spectrum in order to derive a meaningful mean value robust to noise and local

TABLE I
Errors for Reconstruction Using UBD and Different Number of Features for MNF

	B1 (380 nm)				B2 (750 nm)			
Error	RMSE	NRMSE	RMSE (masked)	NRMSE (masked)	RMSE	NRMSE	RMSE (masked)	NRMSE (masked)
UBD	56.02	15.06%	47.42	13.1%	60.79	1.77%	30.55	0.80%
MNF, k = 4	55.94	15.04%	56.74	15.67%	654.1	19.07%	613.92	16.07%
MNF, k = 7	48.81	13.12%	47.31	13.07%	175.52	5.12%	135.44	3.55%
MNF, k = 30	39.73	10.68%	29.85	10.88%	31.18	0.91%	29.85	0.78%

variations. The reference spectra selection step may be replaced in the future by a robust endmember extraction algorithm such as SSEE [18], which also reduces the noise influences by averaging spectra that are both spectrally imilar and spatially close. The proposed algorithm does not use any post-processing through morphological filtering, as it operates pixelwise and may then preserve details in each image element. Experimental results show that UBD provides stable results across all bands, as it automatically intervenes more heavily on bands with low SNR, keeping the informational content of bands with high SNR mostly unaltered. This constitutes an advantage over traditional denoising methods such as MNF, as the optimal number of components to be used in the image reconstruction step for this algorithm is not constant across spectral bands with different SNR. Another interesting aspect is that MNF, like several denoising algorithms for hyperspectral images, is driven by a minimization of the MSE, which has been criticized in the literature due to its poor performance as a visual quality estimator. Our experiments confirm that such criterion on its own is not robust enough to evaluate qualitatively denoising and image reconstruction algorithms for hyperspectral data, both from the informational content and from the perceived visual quality points of view. In [19] the authors expand the structural similarity index (SSIM) [11] from the 2-D case to applications to hyperspectral images, but they do so by simply computing the average value of SSIM across all the spectral bands. The reported experimental results suggest that in the future a similar index, comprising an accurate prediction both for spatial and spectral distortion in hyperspectral images, would represent a valuable contribution to improve the validation of data compression, denoising and sparse reconstruction algorithms for this kind of data.

References

[1] C. Bruce, "Hyspiri mission concept overview and recent ICE and TRL activities," in *Proc. HyspIRI Sci. Workshop*, Oct. 2012.
[2] B. Aiazzi, L. Alparone, A. Barducci, S. Baronti, P. Marcoionni, I. Pippi, and M. Selva, "Noise modelling and estimation of hyperspectral data from airborne imaging spectrometers," *Ann. Geophys.*, vol. 49, no. 1, pp. 1–9, 2006.
[3] T. Kutser, D. C. Pierson, K. Y. Kallio, A. Reinart, and S. Sobek, "Mapping lake CDOM by satellite remote sensing," *Remote Sens. Environ.*, vol. 94, no. 4, pp. 535–540, 2005.
[4] S. C. Johannessen, W. L. Miller, and J. J. Cullen, "Calculation of UV attenuation and colored dissolved organic matter absorption spectra from measurements of ocean color," *J. Geophys. Res.*, vol. 108, no. C9, pp. 1701–1713, 2003.
[5] R. C. Gonzalez and R. E. Woods, *Digital Image Processing*, 3rd ed. Englewood Cliffs, NJ, USA: Prentice-Hall, Aug. 2007.
[6] N. Renard, S. Bourennane, and J. Blanc-Talon, "Denoising and dimensionality reduction using multilinear tools for hyperspectral images," *IEEE Geosci. Remote Sens. Lett.*, vol. 5, no. 2, pp. 138–142, Apr. 2008.
[7] G. Chen and S.-E. Qian, "Denoising of hyperspectral imagery using principal component analysis and wavelet shrinkage," *IEEE Trans. Geosci. Remote Sens.*, vol. 49, no. 3, pp. 973–980, Mar. 2011.
[8] A. A. Green, M. Berman, P. Switzer, and M. D. Craig, "A transformation for ordering multispectral data in terms of image quality with implications for noise removal," *IEEE Trans. Geosci. Remote Sensing*, vol. 26, no. 1, pp. 65–74, Jan. 1988.
[9] U. Amato, R. M. Cavalli, A Palombo, S. Pignatti, and F. Santini, "Experimental approach to the selection of the components in the minimum noise fraction," *IEEE Trans. Geosci. Remote Sens.*, vol. 47, no. 1, pp. 153–160, Jan. 2009.
[10] M. Farzam and S. Beheshti, "Simultaneous denoising and intrinsic order selection in hyperspectral imaging," *IEEE Trans. Geosci. Remote Sens.*, vol. 49, no. 9, pp. 3423–3436, Sep. 2011.
[11] Z. Wang, A. C. Bovik, H. R. Sheikh, and E. P. Simoncelli, "Image quality assessment: From error visibility to structural similarity," *IEEE Trans. Image Process.*, vol. 13, no. 4, pp. 600–612, Apr. 2004.
[12] J. M. P. Nascimento and J. M. Bioucas Dias, "Does independent component analysis play a role in unmixing hyperspectral data?" *IEEE Trans. Geosci. Remote Sens.*, vol. 43, no. 1, pp. 175–187, Jan. 2005.
[13] J. M. Bioucas-Dias, A. Plaza, N. Dobigeon, M. Parente, Q. Du, P. Gader, and J. Chanussot, "Hyperspectral unmixing overview: Geometrical, statistical, and sparse regression-based approaches," *IEEE J. Select. Topics Appl. Earth Observ. Remote Sens.*, vol. 5, no. 2, pp. 354–379, Apr. 2012.
[14] D. Cerra, R. Mueller, and P. Reinartz, "A classification algorithm for hyperspectral images based on synergetics theory," *IEEE Trans. Geosci. Remote Sens.*, to be published.
[15] I. Dopido, M. Zortea, A. Villa, A. Plaza, and P. Gamba, "Unmixing prior to supervised classification of remotely sensed hyperspectral images," *IEEE Geosci, Remote Sens. Lett.*, vol. 8, no. 4, pp. 760–764, Jul. 2011.
[16] G. Mart´ın and A. Plaza, "Spatial-spectral preprocessing prior to endmember identification and unmixing of remotely sensed hyperspectral data," *IEEE J. Select. Topics Appl. Earth Observ. Remote Sens.*, vol. 5, no. 2, pp. 380–395, Apr. 2012.
[17] A. Plaza, P. Martinez, J. Plaza, and R. Perez, "Dimensionality reduction and classification of hyperspectral image data using sequences of extended morphological transformations," *IEEE Trans. Geosci. Remote Sens.*, vol. 43, no. 3, pp. 466–479, Mar. 2005.
[18] D. Rogge, B. Rivard, J. Zhang, A. Sanchez, J. Harris, and J. Feng, "Integration of spatial–spectral information for the improved extraction of endmembers," *Remote Sens. Environ.*, vol. 110, no. 3, pp. 287–303, 2007.
[19] Y. Zhao, J. Yang, Q. Zhang, L. Song, Y. Cheng, and Q. Pan, "Hyperspectral imagery super-resolution by sparse representation and spectral regularization," *EURASIP J. Advances Signal Process.,*, vol. 2011, no. 1, p. 87, 2011.